Determination of isotopic fractionation $\delta^{13}C$ of methane from ground-based FTIR observations performed at the Jungfraujoch

P. Duchatelet[1], E. Mahieu[1], R. Sussmann[2], F. Forster[2], T. Borsdorff[2], P.F. Bernath[3], C.D. Boone[4], K.A. Walker[4,5], M. De Mazière[6] and C. Vigouroux[6]

[1]Institute of Astrophysics and Geophysics of the University of Liège, B-4000 Liège, Belgium
[2]Institute for Meteorology and Climate Research (IMK-IFU), Forschungszetrum Karlsruhe, Garmisch-Partenkirchen, Germany
[3]Department of Chemistry, University of York, Heslington, UK
[4]Department of Chemistry, University of Waterloo, Waterloo, Canada
[5]Department of Physics, University of Toronto, Toronto, Canada
[6]Belgian Institute for Space Aeronomy (BIRA-IASB), Brussels, Belgium
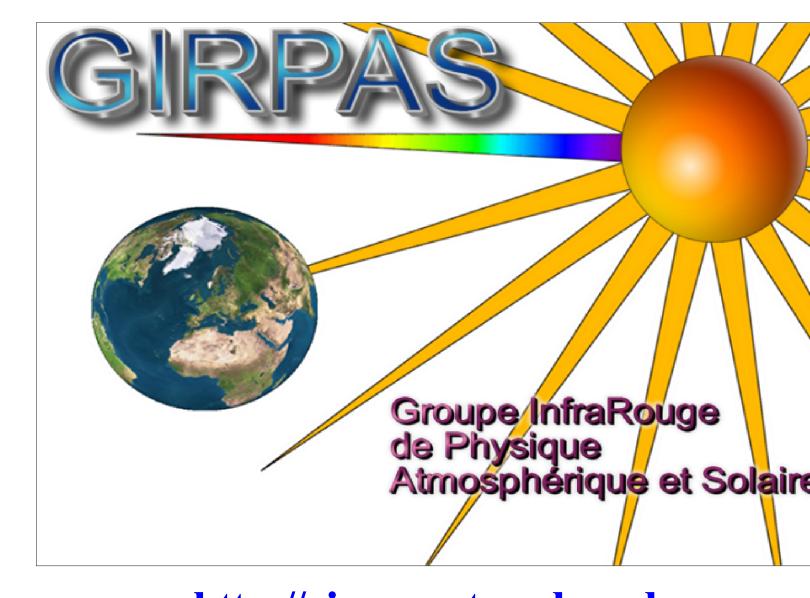
http://girpas.astro.ulg.ac.be

1. INTRODUCTION

Atmospheric methane (CH_4) is a strong greenhouse gas that has important chemical impacts on both the troposphere and the stratosphere. In the troposphere, oxidation of methane is a major regulator of OH and is a source of formaldehyde, carbon monoxide and hydrogen. In the stratosphere, CH_4 plays a central role (i), due to its contribution to the stratospheric water vapor budget, and (ii), as a sink for chlorine atoms which reduces the rate of stratospheric ozone depletion.

Because the different sources of methane (natural and anthropogenic like wetlands, rice paddies, termites, natural gas escape, biomass burning, etc) have distinct $^{13}C/^{12}C$ ratios (usually reported in "delta" notation $\delta^{13}C$), measurements of atmospheric $^{13}CH_4$ content, in addition to those of the main isotopologue ($^{12}CH_4$), can be used to investigate individual source strengths as well as their spatial and temporal distributions. Characterization of the isotopic fractionation of methane is therefore important, for example, to help models constrain estimates of the global methane budget. In this context, different publications concerning the measurement of the $\delta^{13}C$ isotopic ratio, its seasonal cycle and its mid-term trend above various sites in both hemispheres were published during the last twenty years. Experimental techniques used in these papers consist in aircraft or balloon soundings as well as ground-level air sampling. Table 1 gives an overview of $\delta^{13}C$ results published in some recent studies, valid for the northern hemisphere.

To our knowledge, no study about the measurement of the $\delta^{13}C$ isotopic ratio derived from ground-based FTIR spectra has been published to date. This study deals with the possibility of such measurements. Data characterization (e.g. information content and error budget), typical examples of FTIR $\delta^{13}C$ products and comparisons with previous studies are presented here.
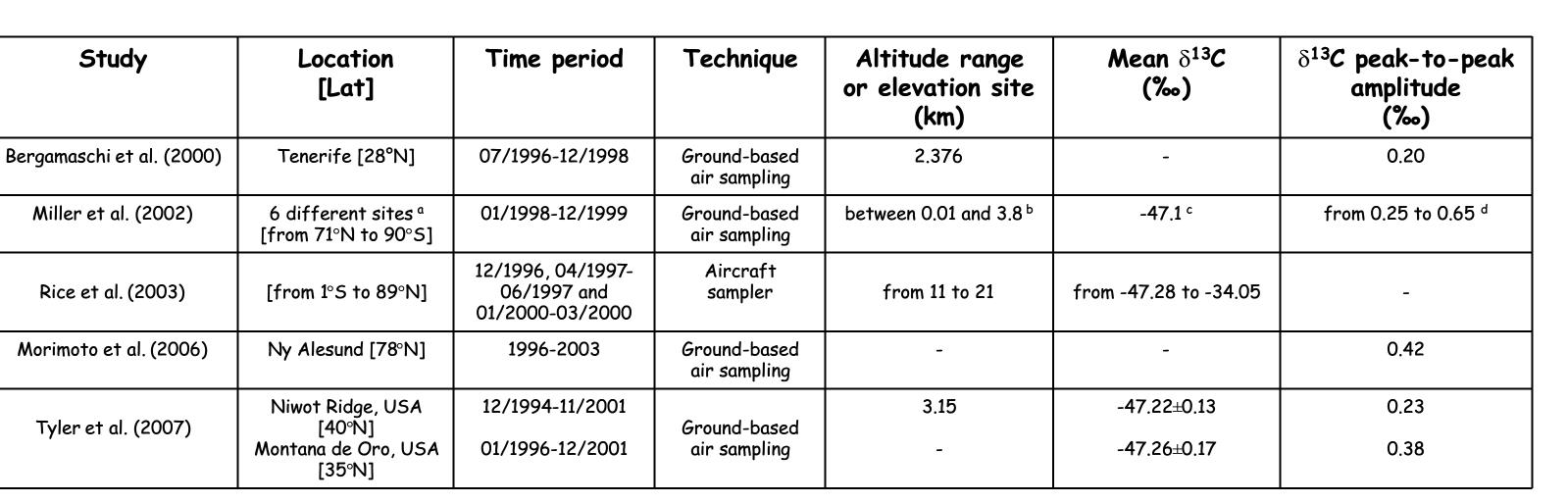
2. RETRIEVAL STRATEGY

All the results produced here have been derived from high resolution solar spectra recorded at the International Scientific Station of the Jungfraujoch (ISSJ, Swiss Alps; 46.5°N latitude, 8.0°E longitude, 3580 m altitude) under clear-sky conditions with a commercial Bruker IFS 120HR spectrometer between January 1998 and December 2008. For $^{12}CH_4$ (resp. $^{13}CH_4$), this represents a database including 3320 (resp. 3704) FTIR spectra recorded over 1170 (resp. 1123) days. For the present work, two sets of spectral microwindows have been defined in order to derive $^{12}CH_4$ and $^{13}CH_4$ total and partial columns. Table 2 summarizes the main characteristics of each set. Third column of Table 2 provides, for each gas, mean DOFS value (and corresponding 1-σ standard deviation) computed over the whole database.

Our methane column retrievals have been performed using the SFIT-2 v3.91 fitting algorithm, a code which has been specifically developed to derive vertical column abundances and volume mixing ratio (VMR) profiles of atmospheric species from ground-based FTIR spectra (Rinsland et al., 1998). The official 2004 version of the HITRAN line parameters compilation (Rothman et al., 2005) has been assumed to simulate $^{13}CH_4$ absorptions during the retrieval procedure. For $^{12}CH_4$, the HITRAN 2004 version including updates derived from laboratory measurements has been used (Duchatelet et al., 2008). The adopted pressure-temperature (p-T) profiles were those provided by the National Centers for Environmental Prediction (NCEP, Washington, D.C.; see http://www.ncep.noaa.gov), specifically computed for the Jungfraujoch site on a daily basis. A priori $^{12}CH_4$ and $^{13}CH_4$ VMR profiles have been provided by IMK-IFU and specifically constructed to match the Jungfraujoch mean tropopause height. For both species, the retrieval strategy is based on a Tikhonov L₁ approach which has been originally developed for $^{12}CH_4$ by Sussmann et al. (2008) [see also contribution by Sussmann et al. to this conference (EGU2009-7869)].

μwindow range (cm⁻¹)	Interfering species	Mean DOFS	Typical PC limits and associated retrieved error
$^{12}CH_4$			
2613.70 - 2615.40	H₂O, CO₂, solar lines		
2650.60 - 2651.30	H₂O, CO₂		
2835.50 - 2835.80	none	2.47 ± 0.20	[3.58 - 7] km (2%)
2903.60 - 2904.03	NO₂		[7 - 17] km (1.5%)
2921.00 - 2921.60	H₂O, NO₂		
$^{13}CH_4$			
1234.04 - 1234.44	CH₄, $^{13}CO_2$, COF₂	1.57 ± 0.29	[3.58 - 18] km (7%)

Table 2 - Selection of microwindows for $^{12}CH_4$ and $^{13}CH_4$ retrievals. For $^{13}CH_4$, all microwindows are simultaneously adjusted during the retrieval procedure. Second column lists the interfering gases included in each microwindow and whose VMR profiles are also scaled during the iterative process. Third column provides, for each methane isotopologue, the mean DOFS value (and corresponding 1-σ standard deviation) computed over the whole time series. Last column provides typical partial column (PC) limits as well as the error characterizing retrieved PC. Total errors affecting our $^{12}CH_4$ and $^{13}CH_4$ total columns are equal to 1% and 6%, respectively.

Study	Location [Lat]	Time period	Technique	Altitude range or elevation site (km)	Mean $\delta^{13}C$ (‰)	$\delta^{13}C$ peak-to-peak amplitude (‰)
Bergamaschi et al. (2000)	Tenerife [28°N]	07/1996-12/1998	Ground-based air sampling	2.376		0.20
Miller et al. (2002)	6 different sites [a] [from 71°N to 90°S]	01/1998-12/1999	Ground-based air sampling	between 0.01 and 3.8 [b]	-47.1 [c]	from 0.25 to 0.65 [d]
Rice et al. (2003)	[from 7.5 to 89°N]	12/1996, 04/1997-06/1997 and 01/2000-03/2000	Aircraft sampler	from 11 to 21	from -47.28 to -34.05	-
Morimoto et al. (2006)	Ny Alesund [78°N]	1996-2003	Ground-based air sampling			0.42
Tyler et al. (2007)	Niwot Ridge, USA [40°N] Montana de Oro, USA [35°N]	12/1994-11/2001 01/1996-12/2001	Ground-based air sampling	3.15	-47.22±0.13 -47.26±0.17	0.23 0.38

[a] Among them, 3 are located in the NH: Point Barrow, Alaska [71°N], Niwot Ridge, Colorado [40°N] and Mauna Loa, Hawaii [19°N].
[b] For the 3 NH sites.
[c] Global average including both hemispheres; the average difference between Point Barrow and the South Pole is 0.6‰.
[d] For the 3 NH sites; peak-to-peak amplitude increases with increasing latitude.

Table 1 - Some recent measurements of $\delta^{13}C$ in the Northern Hemisphere (NH).

Figure 1 - Daily mean $^{12}CH_4$ 6-18 km partial columns time series as observed by the ACE-FTS space instrument (blue and light blue circles) and by FTIR spectrometry at Jungfraujoch (yellow circles). Light blue circles correspond to coincident days between satellite and ground-based data. Top panel reproduces relative differences between FTIR and ACE-FTS data (solid line: mean relative difference; dotted lines: 1-σ standard deviation on the mean).
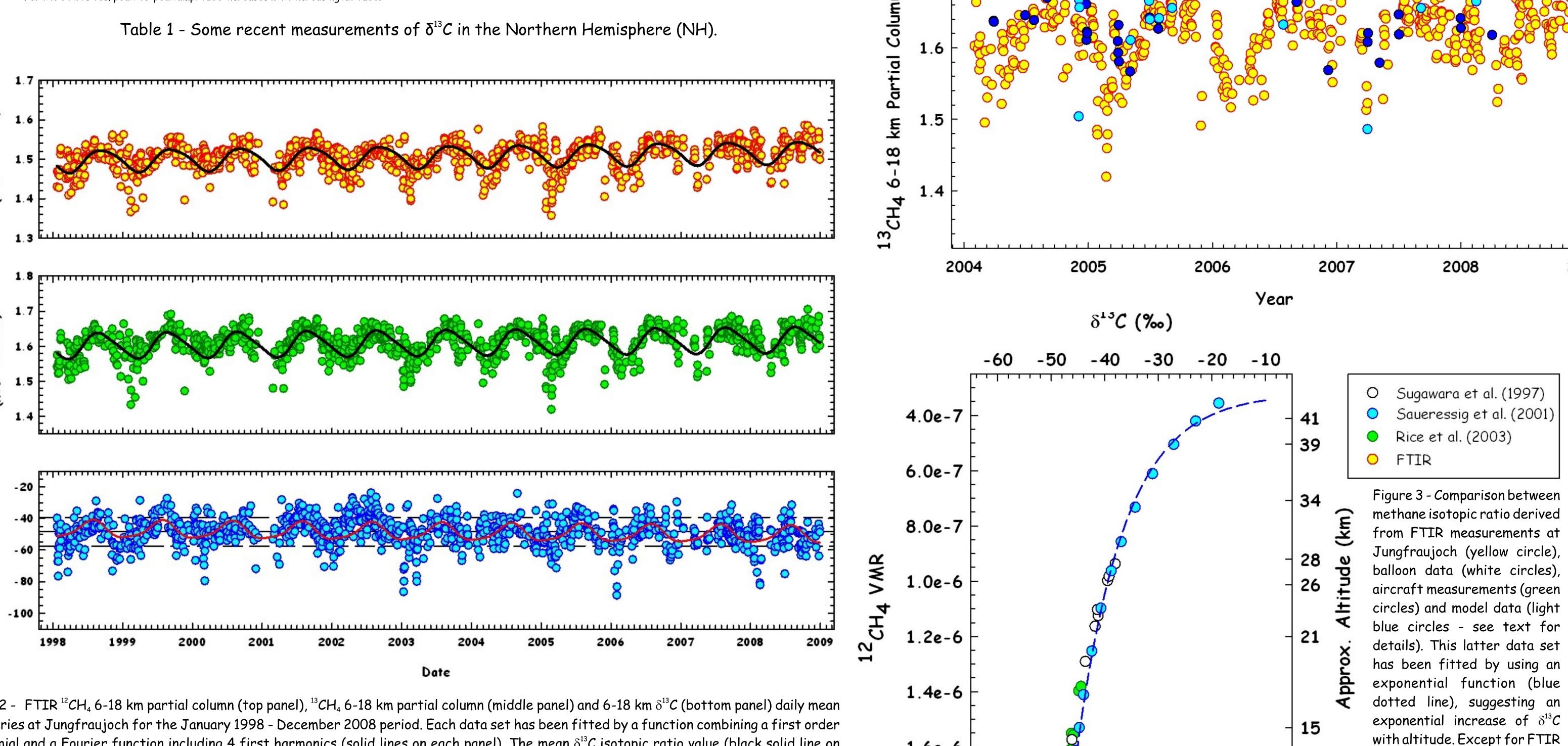

Figure 2 - FTIR $^{12}CH_4$ 6-18 km partial column (top panel), $^{13}CH_4$ 6-18 km partial column (middle panel) and 6-18 km $\delta^{13}C$ (bottom panel) daily mean time series at Jungfraujoch for the January 1998 - December 2008 period. Each data set has been fitted by a function combining a first order polynomial and a Fourier function including 4 first harmonics (solid lines on each panel). The mean $\delta^{13}C$ isotopic ratio value (black solid line on bottom panel; dotted lines correspond to 1-σ standard deviation on the mean) computed over the whole time series is equal to -48.4±9.1 ‰ and is in excellent agreement with mean values reported in the sixth column of Table 1.

Figure 3 - Comparison between methane isotopic ratio derived from FTIR measurements at Jungfraujoch (yellow circle), balloon data (white circles), aircraft measurements (green circles) and model data (light blue circles - see text for details). This latter data set has been fitted by using an exponential function (blue dotted line), suggesting an exponential increase of $\delta^{13}C$ with altitude. Except for FTIR data, all data points have been obtained by digitization of data points included in Figures appearing in references mentionned in the legend.

3. COMPARISONS WITH OTHER DATA SETS

Comparisons of FTIR $^{12}CH_4$ products obtained by applying a Tikhonov L₁ retrieval strategy with satellite data are fully exposed and discussed in Sussmann et al. (2008) [see also contribution by Sussmann et al. to this conference (EGU2009-7869)]. In order to compare our $^{12}CH_4$ products, our daily mean FTIR $^{12}CH_4$ 6-18 km partial columns have been confronted with daily mean values derived from all ACE-FTS space instrument occultations recorded in the [41-51]°N latitudinal belt between February 2004 and July 2008 (Figure 1). This represents a subset of 41 data points (blue circles in Figure 1) which includes 13 coincident days (light blue circles in Figure 1) with FTIR data (yellow circles in Figure 1). Relative differences between FTIR and ACE-FTS time series are reproduced for coincident days on top pannel of Figure 1 (the solid and dotted lines reproduce the mean relative difference and 1-σ standard deviation, respectively). The altitude range adopted for these comparisons (6-18 km) constitutes a good compromise between the altitude range where the ACE-FTS instrument is able to record $^{12}CH_4$ vertical profiles and the sensitivity range of our FTIR retrievals (see last column of Table 2).

Using the relation: $\delta^{13}C = \left(\dfrac{\left[\frac{^{13}CH_4}{^{12}CH_4} \right]}{\left[\frac{^{13}CH_4}{^{12}CH_4} \right]_{ref}} - 1 \right) \cdot 1000$, where the accepted value for the standard ratio $^{13}CH_4/^{12}CH_4$ is equal to 0.0112372 (Platt et al., 2004), $\delta^{13}C$ isotopic ratio time series can be deduced from methane isotopologues FTIR measurements. Figure 2 displays such daily mean time series (for the 1998-2008 time period) derived from FTIR observations performed at Jungraujoch. For the three data sets of Figure 2, a fit function combining a first order polynomial and a Fourier series including first four harmonics has been displayed (solid lines on each panel) and highlights seasonal effects. The mean isotopic ratio value (black solid line on bottom panel; dotted lines correspond to 1-σ standard deviation on the mean) computed over the whole time series is equal to -48.4±9.1 ‰ and agrees well with mean values reported in the sixth column of Table 1. Taking into account error values characterizing our FTIR methane products and reported in Table 2, the error affecting our $\delta^{13}C$ ratios is close to 2%. Figure 3 compares FTIR mean isotopic ratio with previous data obtained at similar latitudes as Jungfraujoch. These consist in stratospheric air samples collected over Japan with a ballon sampler (Sugawara et al., 1997), in UTLS aircraft measurements performed in the [30-60]°N latitudinal belt (Rice et al., 2003) and in stratospheric model data specifically computed for a latitude of 45°N (Saueressig et al., 2001). Error bars affecting FTIR data point are 1-σ standard deviations characterizing mean $^{13}CH_4$ VMR and $\delta^{13}C$ ratio averaged over the whole time period and for altitudes comprised between 6 and 18 km.

4. SEASONAL BEHAVIOR

Data of $^{12}CH_4$ partial columns and $\delta^{13}C$ isotopic ratios (both computed for the 6-18 km altitude range) have also been analyzed in order to study their seasonal behaviors. Long-term time series have been first detrended by substracting the linear contribution derived from fit functions displayed on Figure 2. Then, the residuals have been fitted with a Fourier function including the first four harmonics. Monthly mean values computed from this fitting and brought down to one calendar year are diplayed on Figure 4.

Significant seasonal cycles clearly appear from both panels of Figure 4. Seasonal behavior in $\delta^{13}C$ indicates that, at Jungfraujoch, methane has the most ^{13}C-enriched CH_4 in summer (July-August) and ^{13}C-depleted CH_4 during winter (December-January). This behavior is quite consistent with $\delta^{13}C$ seasonal cycles deduced from previous studies (see the two last columns of Table 3). However, the agreement is not so good when considering peak-to-peak amplitude. As previous studies have found amplitude values which do not exceed 1 ‰ (see last column of Table 1), we found a peak-to-peak amplitude more than 10 times higher. In addition, contrary to previous studies which have observed a $\delta^{13}C$ seasonal cycle out of phase to CH_4 mixing ratios (see Table 3), our $\delta^{13}C$ and $^{12}CH_4$ seasonal cycles are almost in phase, with a time-lag of only 1 to 2 months.

A possible explanation of these two discrepancies could lie in the fact that our FTIR measurements focus on an UTLS atmospheric layer. Seasonal behavior of $\delta^{13}C$ isotopic ratios derived from FTIR methane total columns and FTIR methane tropospheric columns have still to be considered. Reports concerning linear trends affecting our $^{12}CH_4$, $^{13}CH_4$ and $\delta^{13}C$ time series are also under progress. Calculations from numerical models could also be helpful to try to identify sources responsible of $\delta^{13}C$ values observed above Jungfraujoch during the last decade.
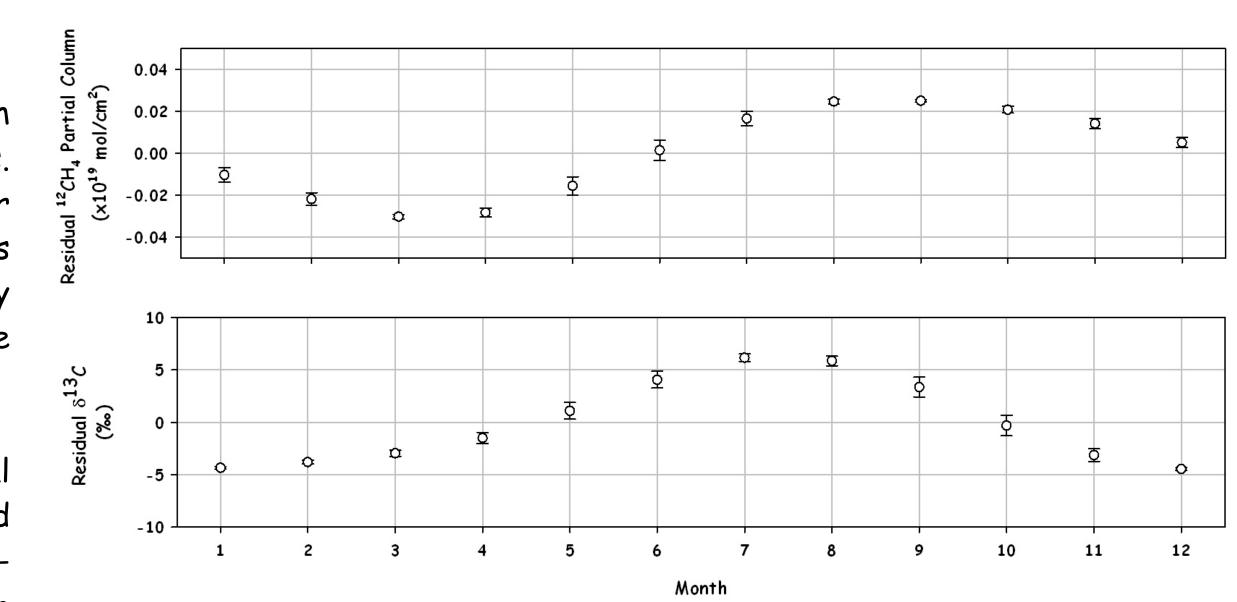

Figure 4 - Mean seasonal behavior of $^{12}CH_4$ 6-18 km partial column and 6-18 km $\delta^{13}C$ isotopic ratio at Jungfraujoch. Data points correspond to monthly means of the Fourier fit (including the first four harmonics) adjusted over the whole detrended time series (see text for details). Error bars are 1-σ standard deviation.

Study	$[^{12}CH_4]_{max}$	$[^{12}CH_4]_{min}$	$[\delta^{13}C]_{max}$	$[\delta^{13}C]_{min}$
Bergamaschi et al. (2000)	November-December	August	June	November-December
Miller et al. (2002)	October-December*	June-August*	April-June*	September-October*
Morimoto et al. (2006)	January-February	July	June	October
Tyler et al. (2007)	October-November	July-August	May-July	October

*Pending of the latitude site.

Table 3 - Period of the year when CH_4 concentration and $\delta^{13}C$ isotopic ratio reach their maximum and minimum values, as deduced from previous studies.

References

Bergamaschi, P. et al., Measurements of the carbon and hydrogen isotopes of atmospheric methane at Izaña, Tenerife: Seasonal cycles and synoptic-scale variations, J. Geophys. Res., 105(D11), 14,531-14,546, 2000.
Duchatelet, P. et al., Impact of different spectroscopic datasets on CH₄ retrievals from Jungfraujoch FTIR spectra, poster presented at the "8" Atmospheric Spectroscopy Applications" meeting (ASA2008), 27 - 30 August 2008, Reims, France, 2008
Miller, J. B. et al., Development of analytical methods and measurements of $^{13}C/^{12}C$ in atmospheric CH₄ from the NOAA Climate Monitoring and Diagnostics Laboratory Global Air Sampling Network, J. Geophys. Res., 107(D13), 4178, doi:10.1029/2001JD000630, 2002.
Morimoto, S. et al., Temporal variations of the carbon isotopic ratio of atmospheric methane observed at Ny Ålesund, Svalbard from 1996 to 2004, Geophys. Res. Lett., 33, L01807, doi:10.1029/2005GL024648, 2006.
Platt, U., et al., Hemispheric average Cl atom concentration from $^{13}C/^{12}C$ ratios in atmospheric methane, Atmos. Chem. Phys., 4, 2393-2399, 2004.
Rice, A. L. et al., Carbon and hydrogen isotopic compositions of stratospheric methane: 1. High-precision observations from the NASA ER-2 aircraft, J. Geophys. Res., 108(D15), 4460, doi:10.1029/2002JD003042, 2003.
Rinsland, C. P. et al., Northern and southern hemisphere ground-based infrared measurements of tropospheric carbon monoxide and ethane, J. Geophys. Res., 103, 28197-28218, 1998.
Rothman, L. S. et al., The HITRAN 2004 molecular spectroscopic database, J. Quant. Spec. and Rad. Transf., 96, 139-204, 2005.
Saueressig, G. et al., Carbon 13 and D kinetic isotope effects in the reactions of CH₄ with O(¹D) and OH: New laboratory measurements and their implications for the isotopic composition of stratospheric methane, J. Geophys. Res., 106(D19), 23,127-23,138, 2001.
Sugawara, S. et al., Vertical Profile of the Carbon Isotopic Ratio of Stratospheric Methane Over Japan, Geophys. Res. Lett., 24(23), 2989-2992, 1997.
Sussmann, R. et al., Satellite validation of column-averaged methane on global scale: ground-based data from 15 FTIR stations versus last generation ENVISAT/SCIAMACHY retrievals, IGAC 10th International Conference, Annecy, France, 7-12 Sep 2008.
Tyler, S. C. et al., Stable isotope ratios in atmospheric CH₄: Implications for seasonal sources and sinks, J. Geophys. Res., 112, D03303, doi:10.1029/2006JD007231, 2007.